

## STATUS OF THE BESSY II FEMTOSECOND X-RAY SOURCE\*

H.-J. Bäcker, J. Bahrtdt, H. A. Dürr, V. Dürr, W. Eberhardt, A. Gaupp, K. Godehusen, K. Hollmack, E. Jaeschke, T. Kachel, S. Khan, D. Krämer, R. Mitzner,

M. Neeb, W. B. Peatman, T. Quast, G Reichardt, M.-M. Richter, M. Scheer, O. Schwarzkopf, F. Senf, G. Wüstefeld (BESSY, 12489 Berlin, Germany)

I. Hertel, F. Noack, W. Sandner, I. Will, N. Zhavoronkov (MBI, 12489 Berlin, Germany)

### Abstract

At the BESSY II storage ring, work is in progress to produce X-ray pulses with 50 fs fwhm duration and tunable energy and polarization. Extensive alterations to the storage ring were made, two beamlines were relocated, a Ti:sapphire laser system was installed, and a THz diagnostics beamline was constructed. The layout of the new femtosecond X-ray source is reviewed and first commissioning results are presented.

### INTRODUCTION

Probing atomic motion and magnetic phenomena on a sub-picosecond time scale with X-rays offers exciting scientific opportunities. The duration of synchrotron radiation pulses is usually limited to tens of picoseconds. At BESSY II, however, operation with a strongly reduced momentum compaction factor has been demonstrated, producing pulses as short as 0.7 ps rms [1]. X-ray pulses of about 20 fs rms (or 50 fs fwhm) duration with linear and circular polarization will be provided by "femtosecond slicing", a technique proposed [2] and experimentally demonstrated [3] at the Advanced Light Source in Berkeley. As sketched in figure 1, a femtosecond laser pulse co-propagates with an electron bunch in a wiggler ("modulator"), modulating the energy of electrons in the short overlap region. The off-energy electrons are transversely displaced by a bending magnet in order to extract the short component of radiation emitted in a subsequent undulator ("radiator"). Here, the photon flux is limited by the repetition frequency of the laser, 1-10 kHz for the required pulse energy of 1-2 mJ. On the other hand, the natural synchronization between laser and X-ray pulses allows to exploit the full time resolution in pump-probe applications, while bunch jitter of the order of 1 ps limits the resolution for non-laser based techniques.

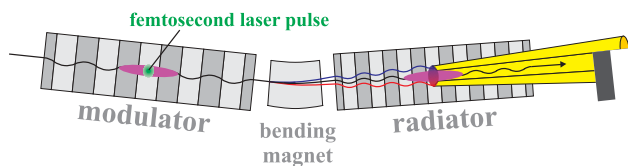


Figure 1: The principle of short-pulse generation by energy modulation of electrons with a femtosecond laser pulse.

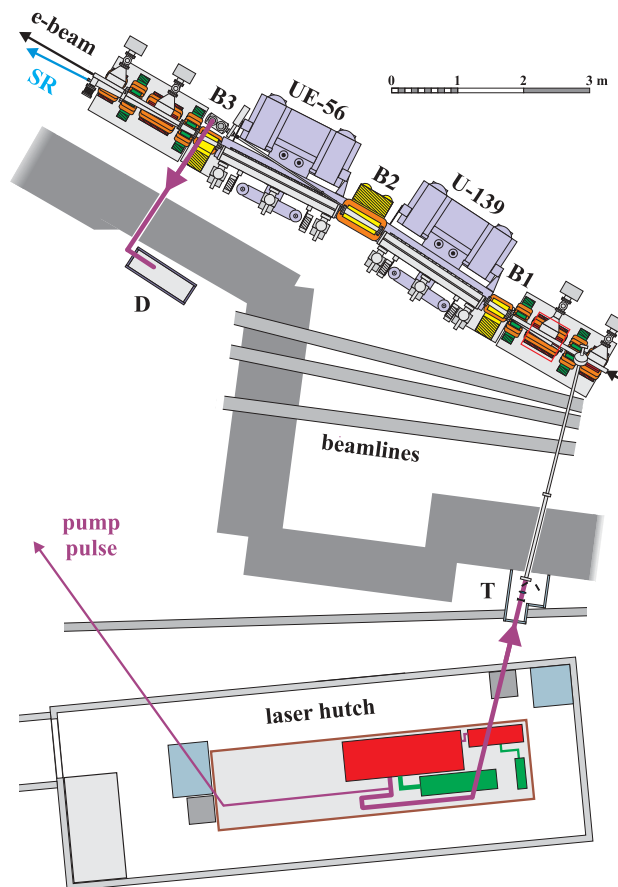


Figure 2: Overview of the femtosecond X-ray source. A laser hut outside the storage ring tunnel contains a Ti:sapphire oscillator and amplifier (red) with respective pump lasers (green). The main pulse is focussed by a telescope (T) and enters the storage ring vacuum, while a small fraction will be sent as pump pulse to the experiment. Modulator (U-139) and radiator (UE-56) are enclosed by a chicane of three bending magnets B1 ( $3.32^\circ$ ), B2 ( $6.40^\circ$ ) and B3 ( $3.08^\circ$ ). Laser and U-139 radiation are directed to a diagnostics station (D) above the ring tunnel.

### HARDWARE INSTALLATION

The layout (figure 2 and [4]) is intended to ensure minimum pulse duration and minimum background. The temporal characteristics of the laser pulse is preserved in the electron distribution by placing the modulator and radiator in the same straight section. To minimize background, the energy-modulated electrons are displaced by a large angle

\* Funded by the Bundesministerium für Bildung und Forschung and by the Land Berlin. Contact: Shaukat.Khan@bessy.de

such that their radiation cone does not overlap with the radiation from the bunch core, which can be blocked by an aperture. This way, focussing elements between source and aperture, which would cause intolerably large background due to non-specular reflection, are avoided. This separation concept was verified by measuring the angular characteristics of the radiator over an intensity range of 7 decades [4]. The radiator (UE-56) is an elliptical undulator (30 periods of length 56 mm) providing linear as well as circular polarization.

In March 2003, the original UE-56 double undulator was removed and its downstream part reinstalled on a new support structure. In November 2003, a liquid-nitrogen cooled Ti:sapphire laser system [5] was installed, providing a pulse energy up to 2.8 mJ at 1 kHz (alternatively 1.8 mJ at 2 kHz). In March 2004, the bending magnets shown in figure 2 were installed, and nine meters of vacuum vessel were replaced, including two aluminium insertion device chambers [6]. The modulator (U-139), a newly constructed planar wiggler (10 periods of length 139 mm) was installed. In the new configuration, the UE-56 axis deviates from the original beam axis and two existing beamlines had to be relocated. Their optical design was modified and an additional beamline was added for femtosecond applications. For diagnostics purposes, a dedicated THz beamline was constructed 12 m downstream of the modulator.

Laser and wiggler radiation are incident on a water cooled copper mirror where the bulk of wiggler radiation (1 kW at a beam current of 250 mA) is absorbed. The remaining light is directed to a diagnostics station above the storage ring tunnel.

## COMMISSIONING EXPERIENCE

Extensive hardware alterations to the storage ring (those mentioned above and others) required recommissioning of the storage ring in April 2004. By the end of April, laser-electron interaction was observed the very first time the laser beam was injected (figure 3, top), and initial experiments were performed with single-bunch fills. Meanwhile, parasitic experiments are carried out with a single bunch of 3-5 mA added to a multi-bunch fill of 250 mA. In the commissioning phase, a single bunch is favored to enhance the THz signal that monitors the laser-electron interaction (see below). For later applications, however, a bunch should not be selected at a rate exceeding the longitudinal damping rate of  $125 \text{ s}^{-1}$ .

The spatial overlap of laser and electron beam is established by focussing a CCD camera into the interaction region and observing the laser spot together with synchrotron radiation, either from the modulator or from the adjacent bending magnets. Changing the camera focus reveals angular misalignment. With the Ti:sapphire oscillator synchronized to the storage ring rf system, temporal overlap is achieved by shifting the rf phase such that photodiode signals from laser and wiggler pulses coincide. Scanning the rf phase while observing the THz signal yields a high-

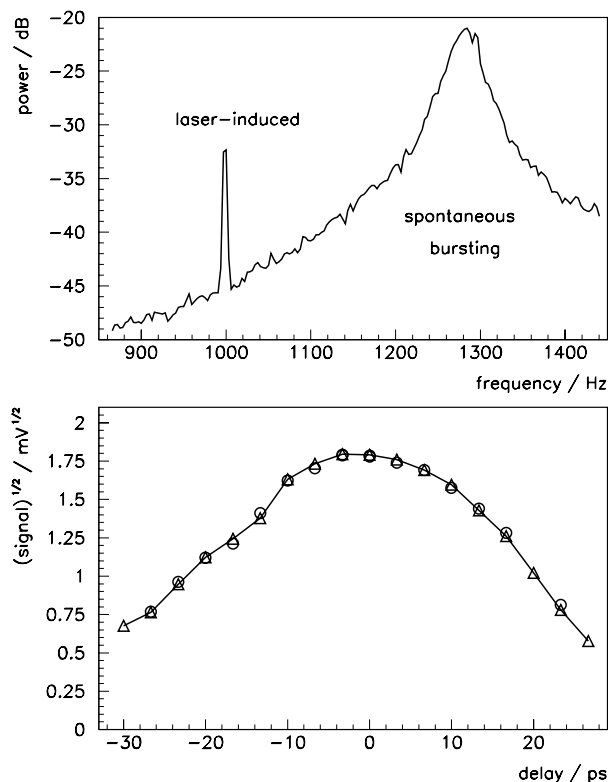


Figure 3: Top: the first THz signal at 998.8 Hz, the repetition rate of the laser, was observed on top of coherent synchrotron radiation bursts [7]. Bottom: The square root of the THz intensity as function of laser pulse delay shows the longitudinal bunch profile. The forward and backward scan are distinguished by symbols.

resolution image of the longitudinal bunch profile (figure 3, bottom). The modulation of the electron energy under the influence of the laser has been demonstrated by two independent methods:

- Observation of enhanced radiation in the THz regime,
- Lifetime measurements while scraping the beam.

### THz Radiation

At a bending magnet 12 m downstream of the modulator, electrons with an energy modulation of  $\Delta E/E \leq 0.01$  are longitudinally displaced by max. 0.15 mm (0.5 ps), leaving a hole in the longitudinal electron distribution (figure 4). The coherent synchrotron radiation in the THz region as a consequence of this hole is an excellent tool for online diagnostics of the laser-electron interaction, and is discussed in more detail in [8]. The interaction is usually optimized observing the integral of the spectrum up to  $\approx 60 \text{ cm}^{-1}$ , which scales with the square of the number of electrons (or missing electrons in the case of a hole). As shown by the simulation result in figure 4b and c, the shape of the hole reflects changes of spatial overlap, e.g. by misalignment or by the laser waist being too small. The THz signal is ex-

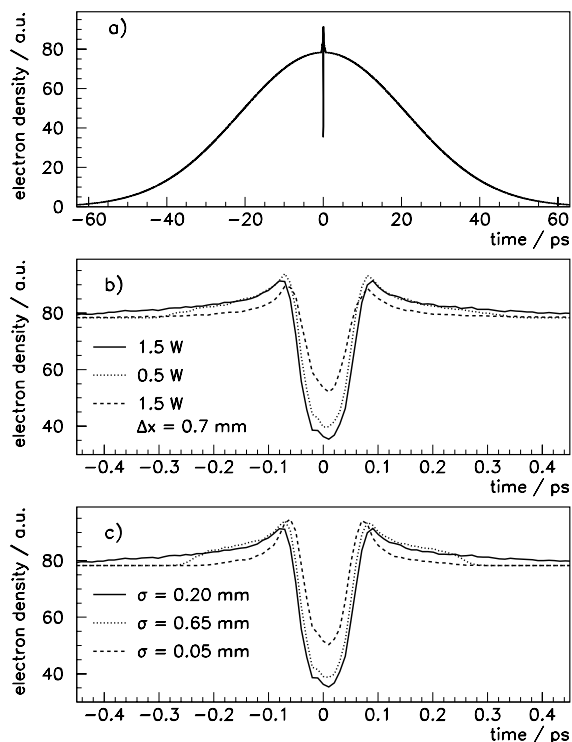


Figure 4: a) Bunch profile with a "hole" due to energy modulation. b) Simulated electron distribution for different laser power (1.5 W and 0.5 W) and with horizontal misalignment  $\Delta x$ . c) Simulated electron distribution under variation of the rms laser waist size  $\sigma$ .

pected to be less sensitive to changes retaining the number of electrons such as reduction of laser power or the laser waist being too large.

### Scraper Experiments

The energy modulation  $\Delta E/E$  at a position with optical functions  $\beta_x$ ,  $\alpha_x$ ,  $\gamma_x$ , dispersion  $D$  and  $D' = dD/ds$  excites a betatron oscillation. With a scraper positioned at a distance of  $\Delta x$  from the beam center, electrons contribute to the loss rate (i.e. the inverse beam lifetime) if

$$\Delta x \leq \Delta E/E \sqrt{\beta_x^S \sqrt{\gamma_x D^2 + 2\alpha_x D D' + \beta_x D'^2}}, \quad (1)$$

where the horizontal beta function is  $\beta_x^S$  and the dispersion is zero at the scraper location. In a recent single-bunch experiment, a scraper was moved close to the beam while alternating between laser on and off every 10 s and recording the loss rate with a sensitive photodiode [9], as shown in figure 5. The dashed line represents a calculated loss rate combining different contributions: constant (vertical Coulomb scattering, bremsstrahlung in dispersion-free regions), depending on the scraper position (horizontal Coulomb scattering, bremsstrahlung in dispersive regions, quantum lifetime), on the beam current (Touschek scattering in dispersion-free regions), and on both (Touschek scat-

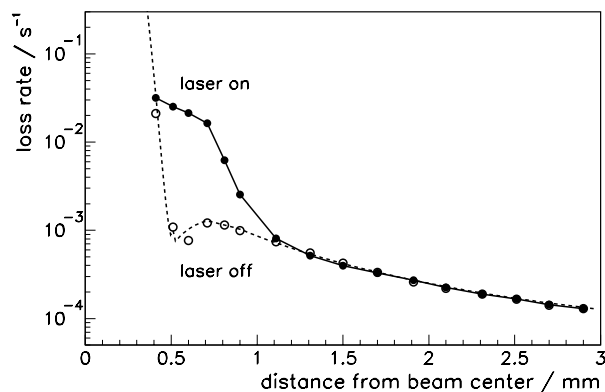


Figure 5: Electron loss rate as function of horizontal scraper position with and without laser-induced energy modulation.

tering in dispersive regions). The loss rate difference at a given scraper position divided by the laser repetition frequency (1 kHz) yields the fraction of electrons exceeding an energy modulation given by equation 1. In the example of figure 5, obtained with reduced laser power, the maximum energy modulation is about 0.5 % of the beam energy.

Presently (June 2004), the laser-electron interaction is being optimized and characterized, which is also of interest in the context of seeded free electron lasers. The next commissioning step will be the detection of undulator radiation from energy modulated electrons behind the UE-56 plane-grating monochromator. The required shifting of the electron orbit by 1 mrad in the UE-56 region during regular user operation is currently being tested.

### ACKNOWLEDGEMENTS

We wish to express our gratitude to all BESSY colleagues contributing to this project. We thank S. Backus, D. Müller, K. Read (KMLabs, Boulder) for their friendly and efficient support. Helpful discussions with P. Heimann, R. Schoenlein, A. Zholents (LBNL, Berkeley), R. Abela, G. Ingold, A. Streun (SLS, Villigen) and hardware support by T. Lohse (HU, Berlin) are gratefully acknowledged.

### REFERENCES

- [1] G. Wüstefeld et al., this conference (EPAC'04).
- [2] A. A. Zholents, M. S. Zolotarev, PRL 76 (1996), 912.
- [3] R. W. Schoenlein et al., Science 287 (2000), 2237.
- [4] S. Khan et al., PAC'03, Portland (2003), 836.
- [5] Kapteyn-Murnane Laboratories Inc. MTS oscillator and HAP-AMP amplifier, Coherent Verdi V5, Quantronix 527DQE-S.
- [6] E. Trakhtenberg et al., PAC'03, Portland (2003), 830.
- [7] M. Abo-Bakr et al., PAC'03, Portland (2003), 3023.
- [8] K. Holldack et al., this conference (EPAC'04).
- [9] The photodiode signal was made available by G. Brandt and R. Klein (PTB, Berlin).